Electronic Supplementary Material (ESI) for Inorganic Chemistry Frontiers.

Supporting Information

A mitochondrial-targeting iridium(III) complex for H_2O_2-responsive and oxidative stress amplified two-photon photodynamic therapy

Xinxing Liao,[a,‡] Jinchao Shen,[a,‡] Weijun Wu,[a,‡] Shi Kuang,[a] Mingwei Lin,[a] Johannes Karges,[b] Zilong Tang, *[c] and Hui Chao, *[a,c]

[a] *MOE Key Laboratory of Bioinorganic and Synthetic Chemistry, School of Chemistry, Sun Yat-Sen University, Guangzhou 510006, China. E-mail: ceschh@mail.sysu.edu.cn*

[b] *Department of Chemistry and Biochemistry, University of California, San Diego, 9500 Gilman Drive, La Jolla, CA 92093, United State*

[c] *MOE Key Laboratory of Theoretical Organic Chemistry and Functional Molecule, School of Chemistry and Chemical Engineering, Hunan University of Science and Technology, Xiangtan, 400201, China. E-mail: zltang@hnust.edu.cn*

[‡] These authors contributed equally to this work.

Supporting Figures and Tables

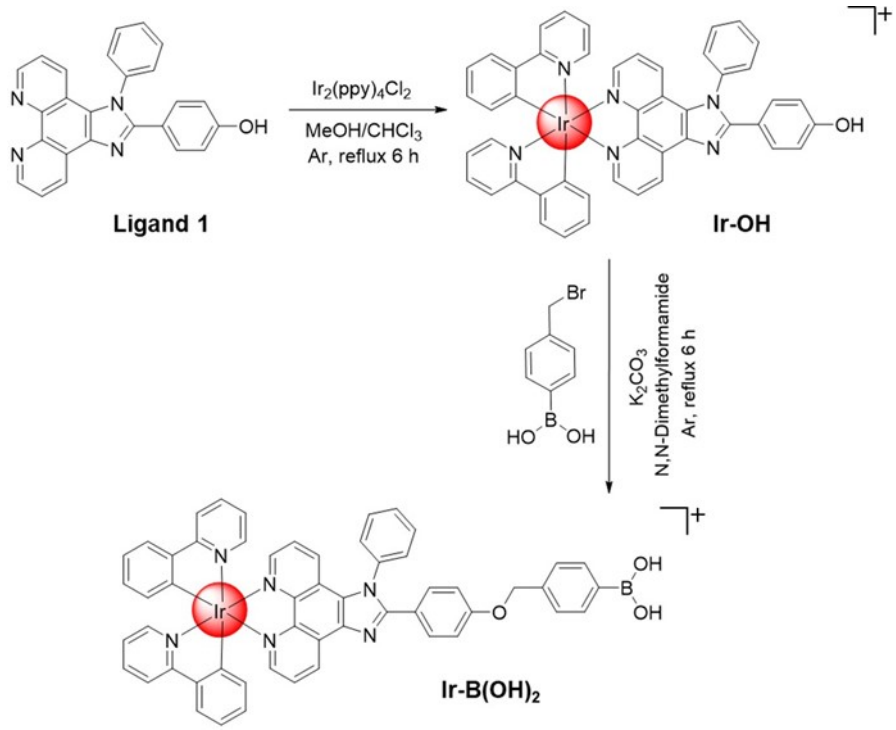

Scheme S1. Synthetic route of **Ir-B(OH)$_2$**.

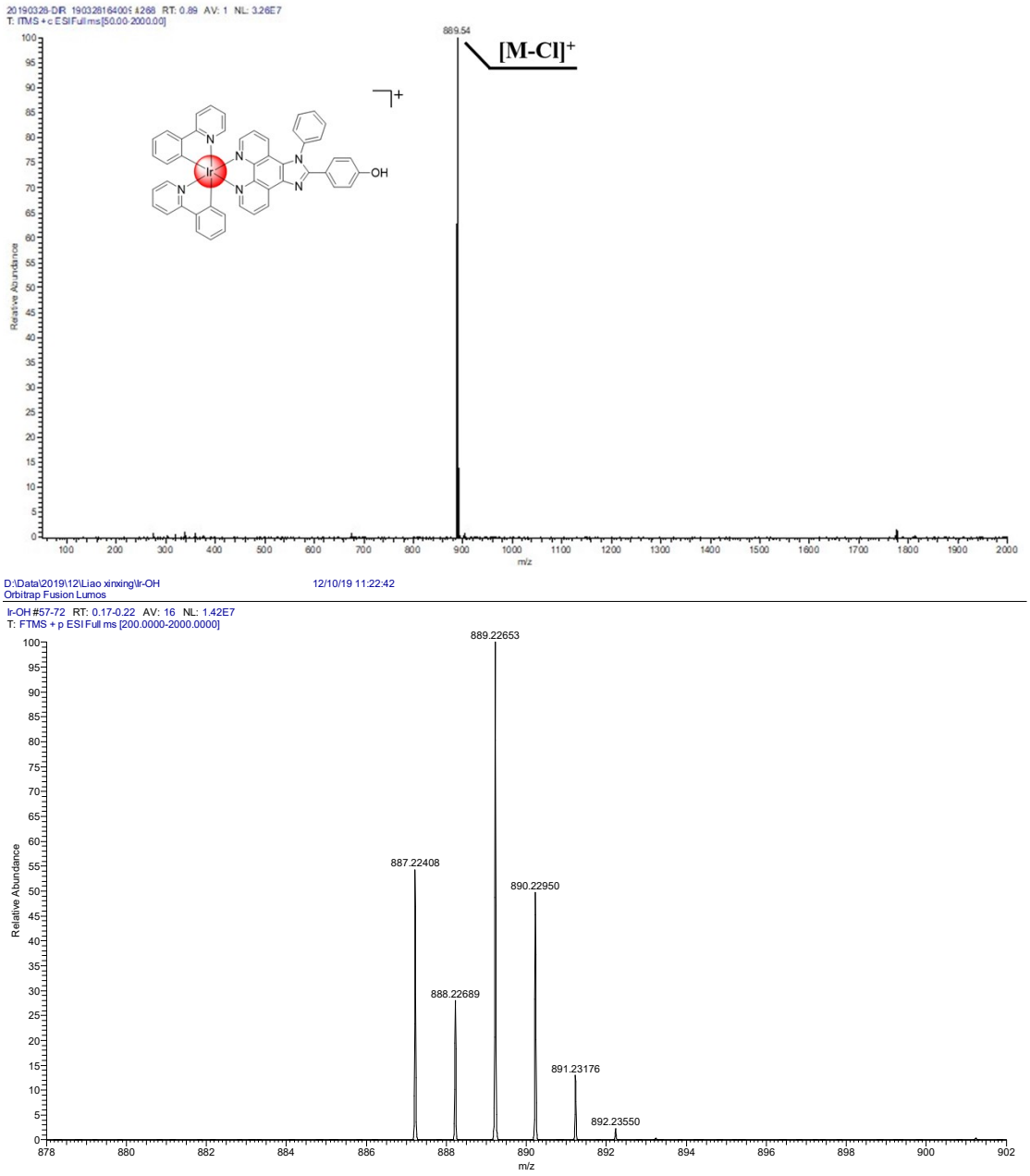

Figure S1. ESI-MS spectrum and HRMS spectrum of **Ir-OH**.

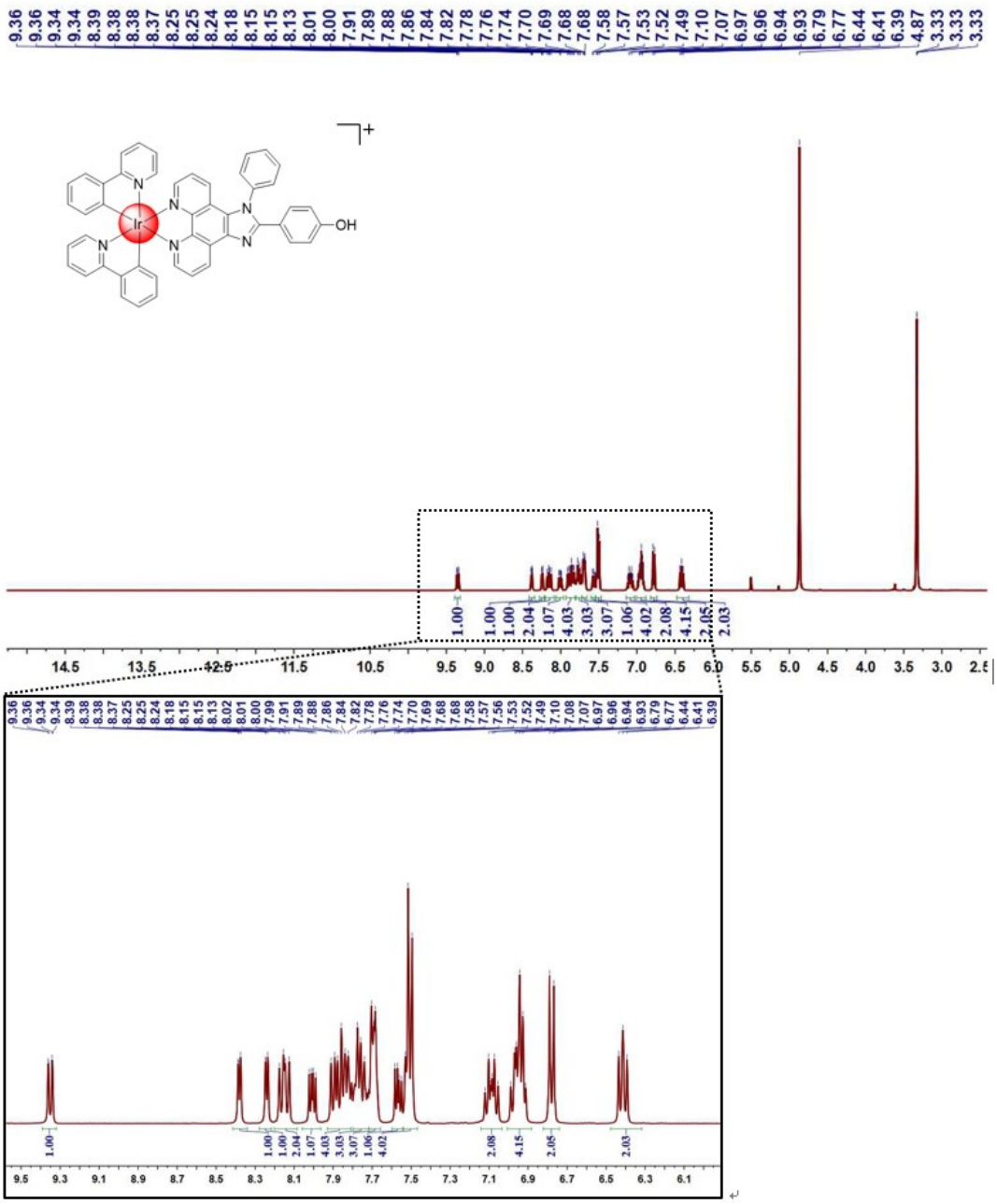

Figure S2. ^{1}H NMR spectrum of **Ir-OH**.

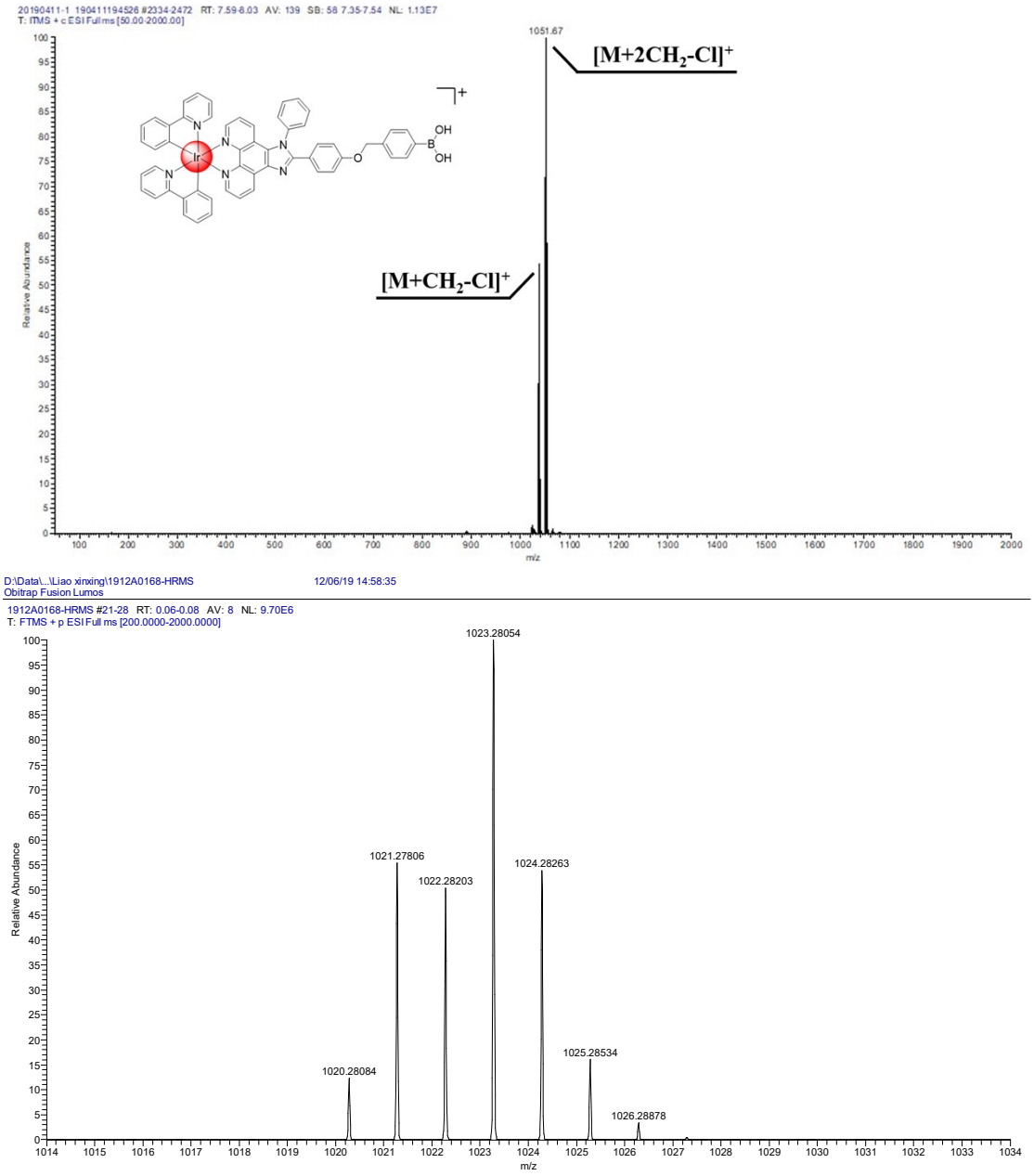

Figure S3. ESI-MS spectrum and HRMS spectrum of **Ir-B(OH)$_2$**.

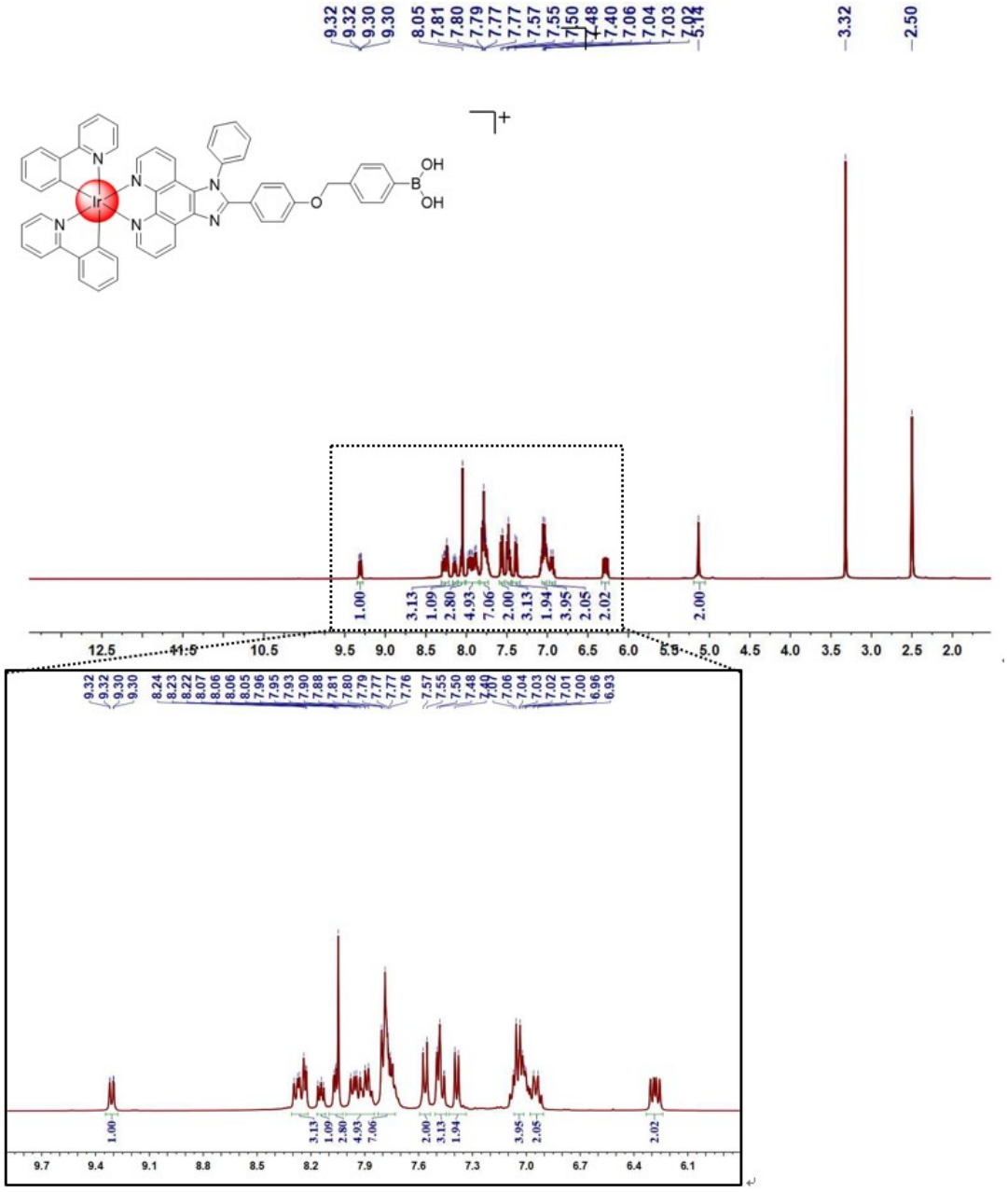

Figure S4. ^{1}H NMR spectrum of **Ir-B(OH)$_2$**.

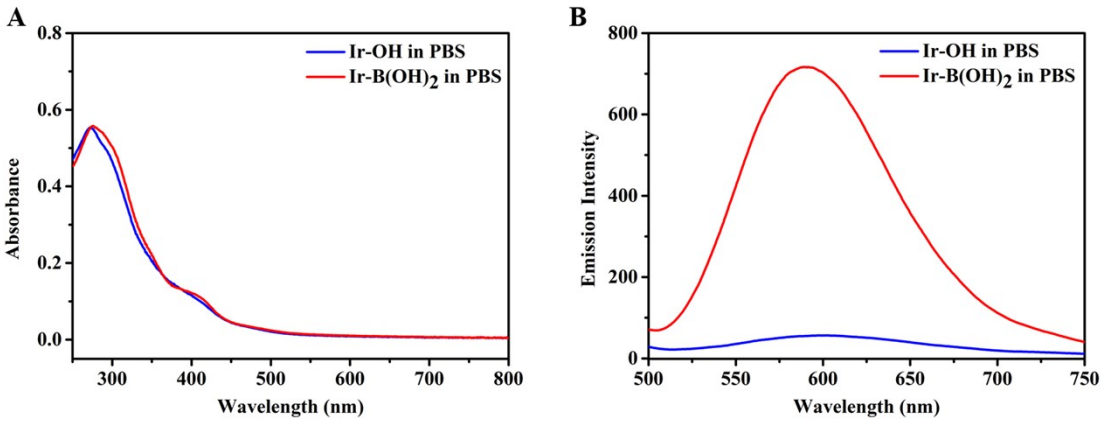

Figure S5. UV-Vis absorption spectra (A), and emission spectra (B) of **Ir-OH** (10 μM), and **Ir-B(OH)$_2$** (10 μM) in PBS.

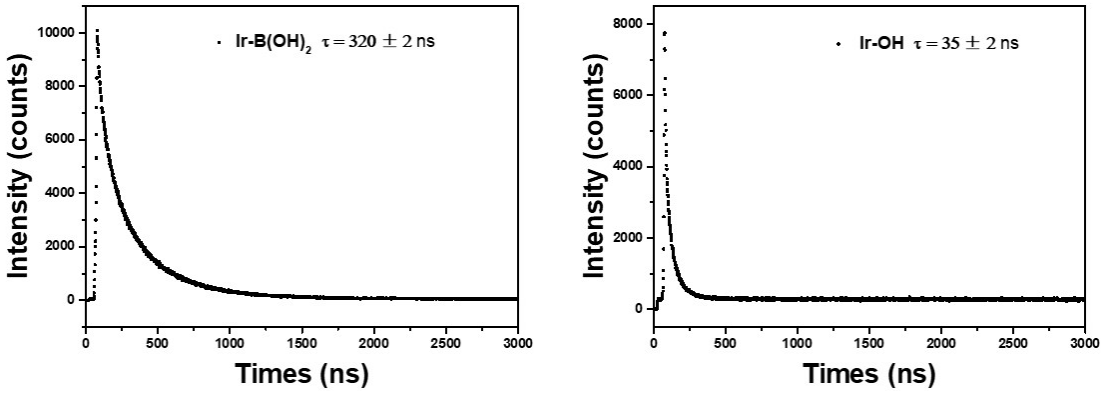

Figure S6. Luminescence lifetime spectra of **Ir-OH** (10 μM), and (B) **Ir-B(OH)$_2$** (10 μM) in PBS.

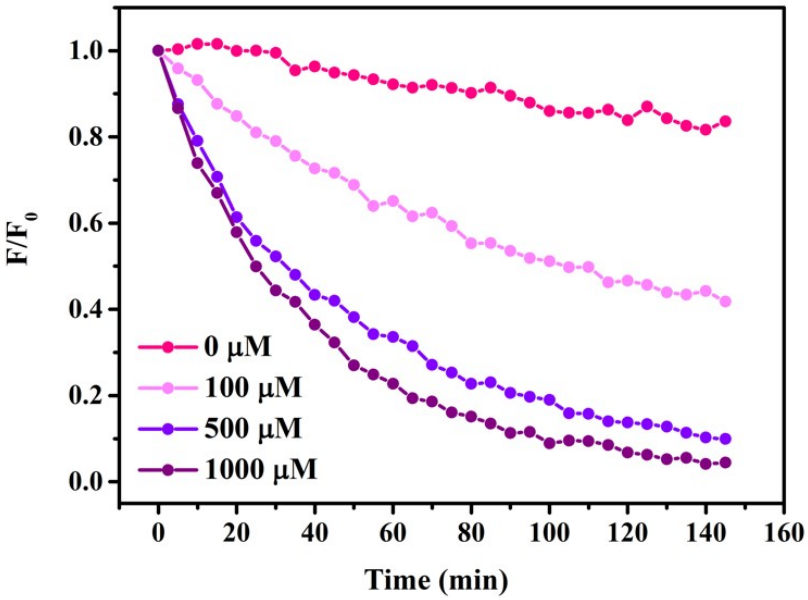

Figure S7. Monitoring of changes in the emission intensity at 589 nm of **Ir-B(OH)$_2$** (2.0 μM) upon treatment with various H_2O_2 concentrations at various time points.

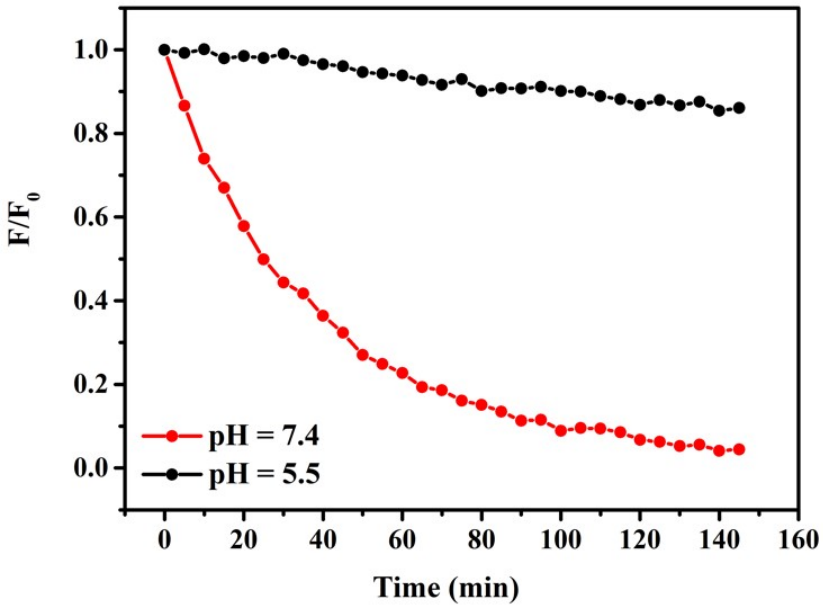

Figure S8. Monitoring of changes in the emission intensity at 589 nm of **Ir-B(OH)$_2$** (2.0 μM) upon treatment with H_2O_2 at various time points under physiological (pH = 7.4) or acidic conditions (pH = 5.5).

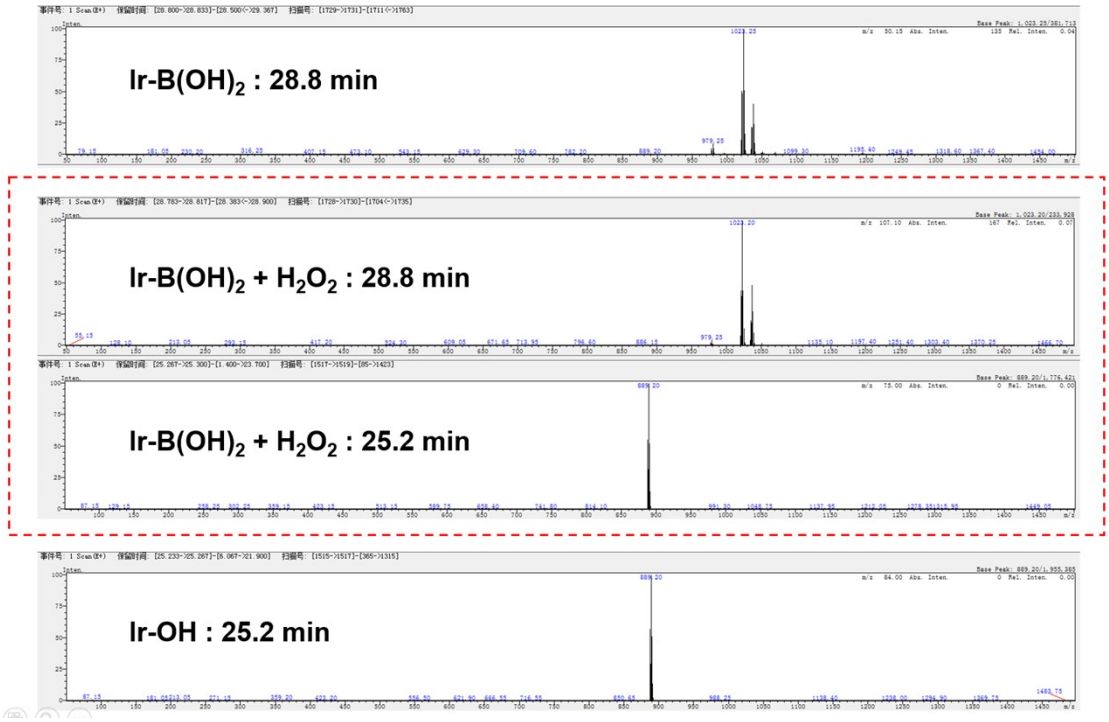

Figure S9. Mass spectrum at the corresponding retention time upon incubation of **Ir-B(OH)$_2$** with H_2O_2.

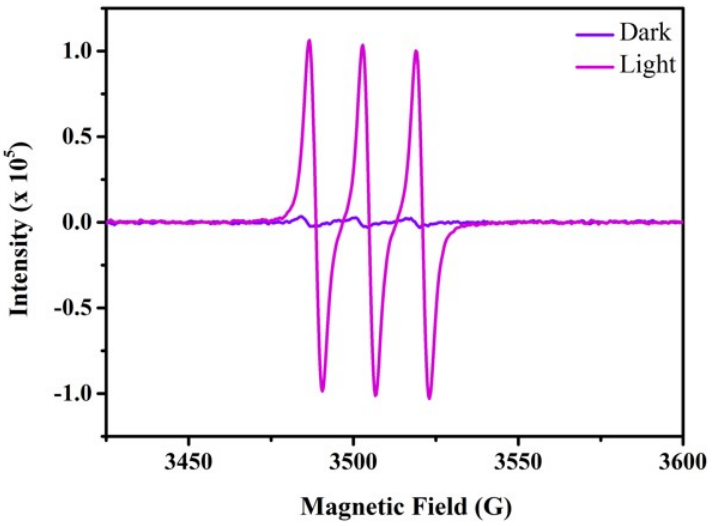

Figure S10. Electron spin resonance spectrum of **Ir-B(OH)$_2$ (**2.0 µM) upon incubation of 2,2,6,6-tetramethylpiperidine and exposure to a 405 nm irradiation (20 mW cm^{-2}, 300 s).

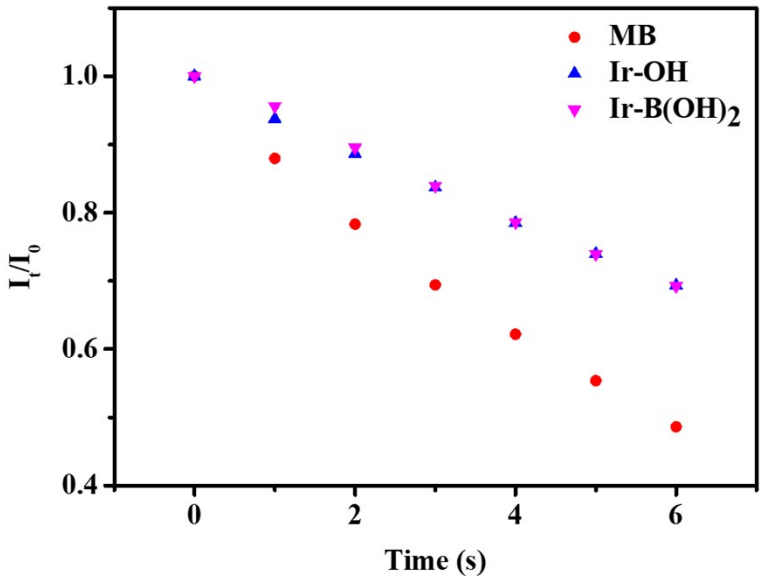

Figure S11. Changes in the absorbance at 411 nm (absorption of 1,3-diphenylisobenzofuran (DPBF)) upon incubation of the metal complexes **Ir(OH)** or **Ir-B(OH)$_2$** with the $^1O_2$ scavenger DPBF. MB was used as the standard.

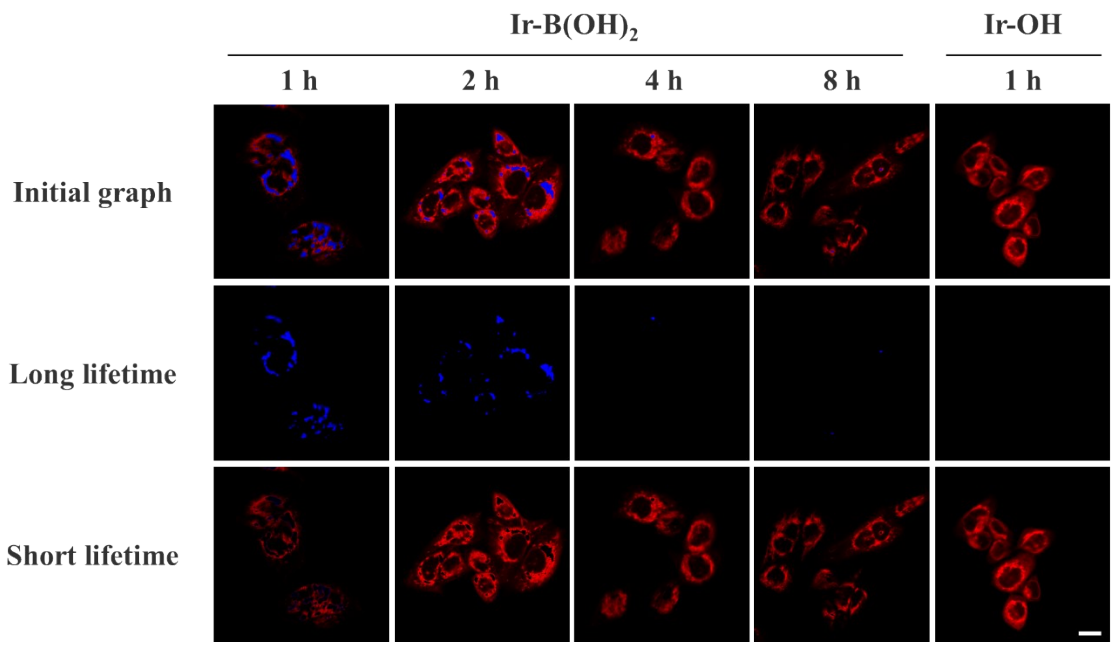

Figure S12. Phosphorescence lifetime images of AGS cells incubated with **Ir-B(OH)$_2$** (0.5 μM) for 1, 2, 4, 8 h or **Ir-OH** (0.5 μM) for 1h (λ_{ex} = 730 nm). Scale bar: 10 μm.

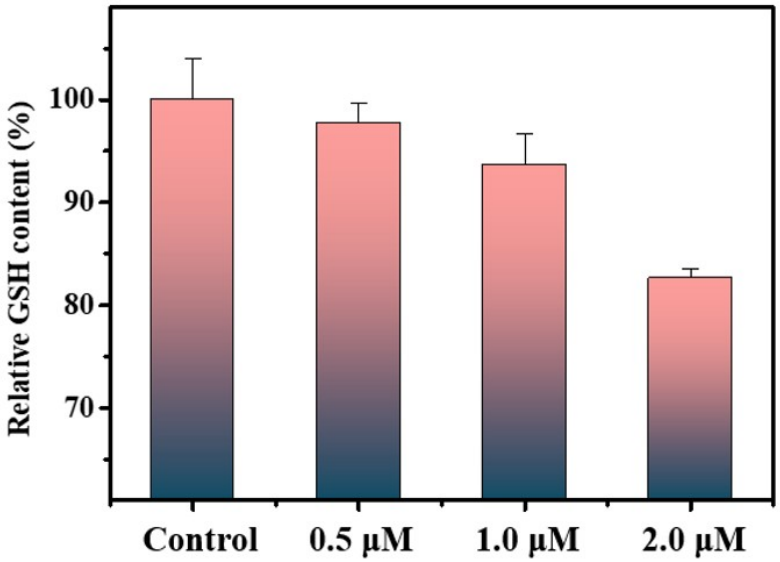

Figure S13. Relative intracellular GSH level of AGS cells upon treatment with various concentrations of **Ir-B(OH)$_2$**.

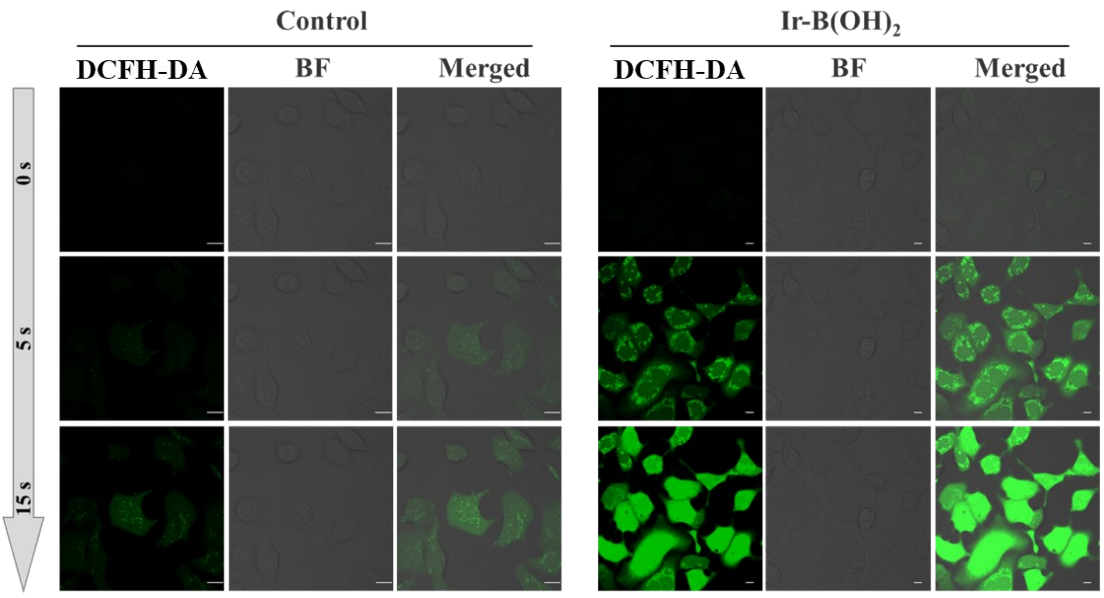

Figure S14. Fluorescence images of AGS cells incubated with **Ir-B(OH)$_2$** (0.5 μM), stained with 2,7-dichlorodihydrofluorescein diacetate (10 μM, λ_{ex} = 488 nm, λ_{em} = 510 ± 10 nm) and exposure to a laser irradiation (405 nm, 20 mW cm^{-2}, 300 s). Scale bar: 10 μm.

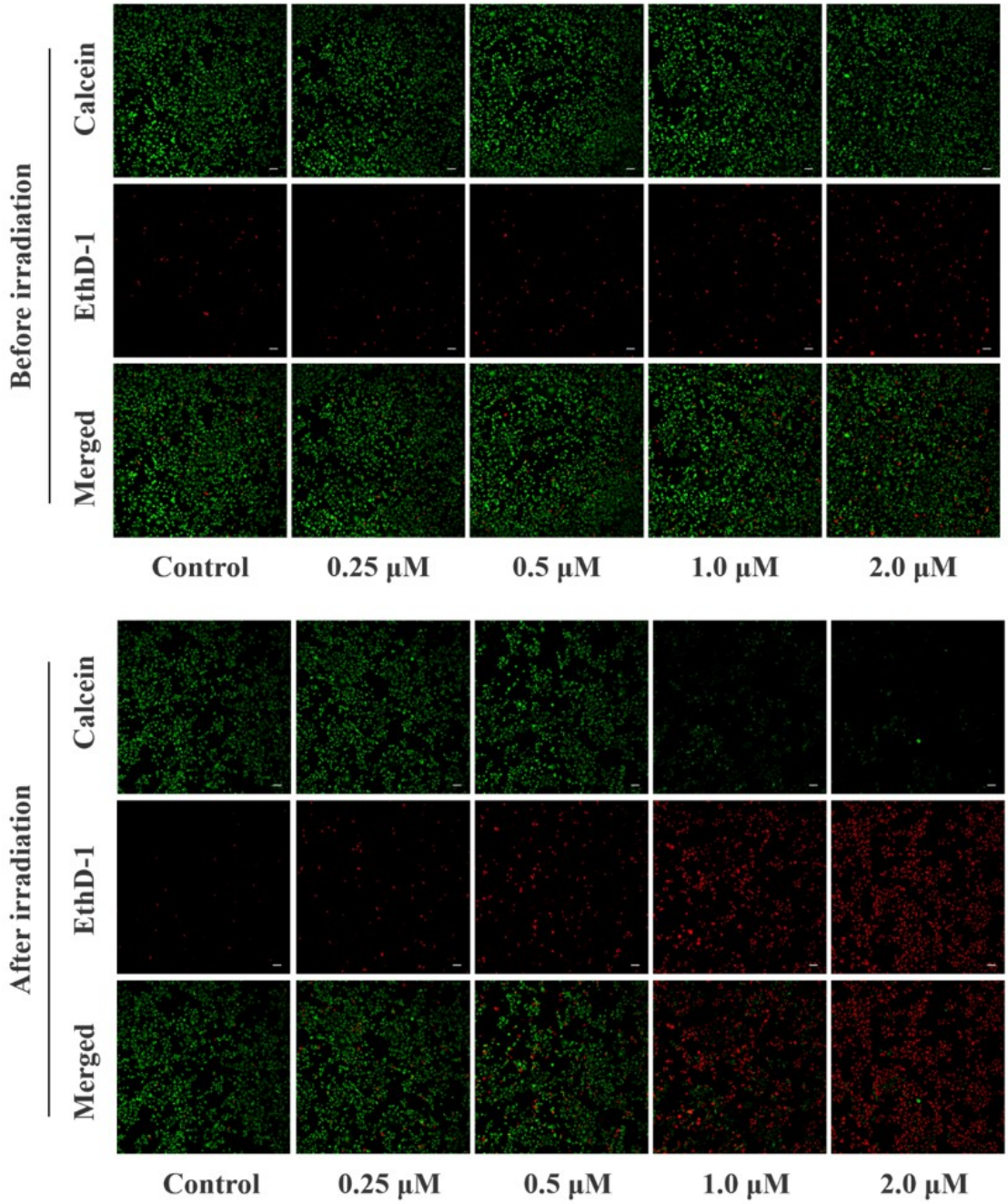

Figure S15. Fluorescent microscopy images of AGS cells incubated with **Ir-B(OH)$_2$** before and after a 405 nm laser (20 mW cm^{-2}, 300 s) irradiation. Afterwards, the cells were stained with Calcein-AM/EthD-1 (Calcein-AM for live cells, 2μM, λex = 488 nm, λem = 510 ± 10 nm; EthD-1 for dead cells, 4 μM, λex = 543 nm, λem = 610 ± 10 nm nm). Scale bar = 100 μm.

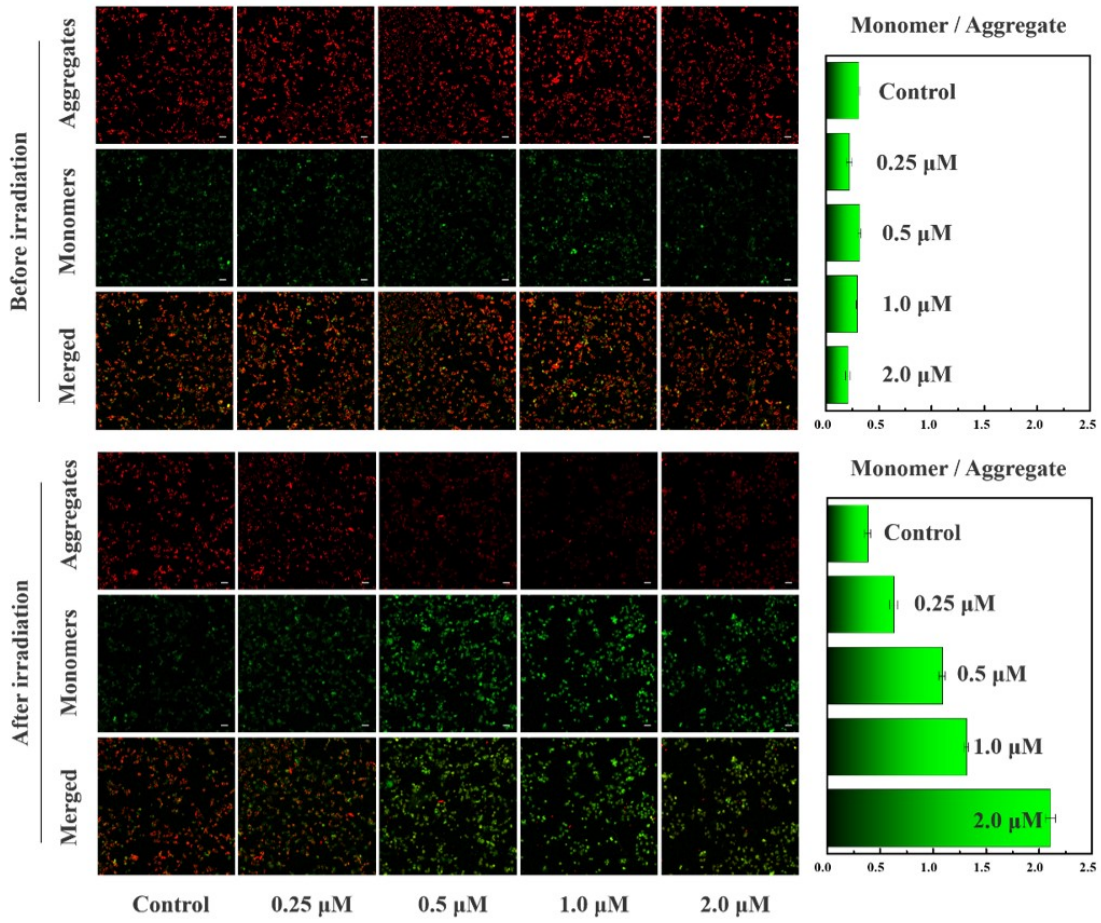

Figure S16. Confocal microscopy images upon incubation of **Ir-B(OH)$_2$** and JC-1 in AGS cells before or after a 405 nm laser (20 mW cm^{-2}, 300 s) irradiation. The JC-1 monomer/aggregate ratio is indicative for the mitochondrial membrane potential. Monomer: λ_{ex} = 488 nm, λ_{em} = 510 ± 10 nm, Aggregate: λ_{ex} = 543 nm, λ_{em} = 610 ± 10 nm, Scale bar = 50 μm.

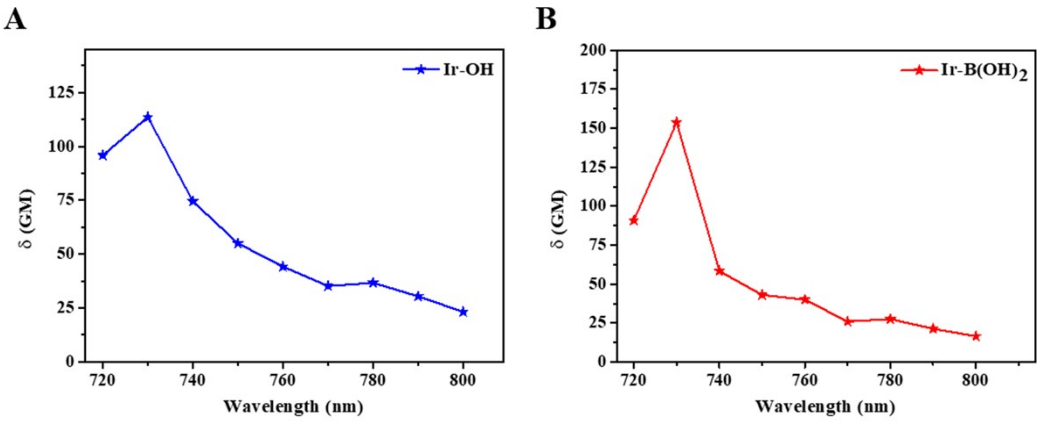

Figure S17. Two-photon absorption spectra of (A) **Ir-OH** (1 mM), and (B) **Ir-B(OH)$_2$** (1 mM)**.**

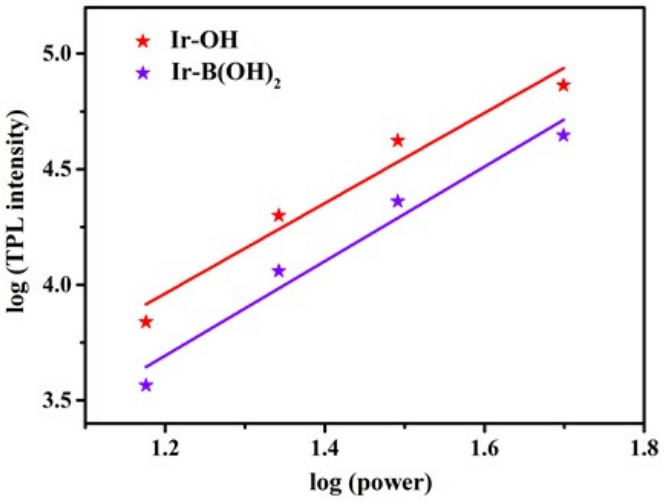

Figure S18. Laser power in dependence of relative two-photo induced phosphoresce intensity of **Ir-OH**(1 mM), and **Ir-B(OH)$_2$** (1 mM).

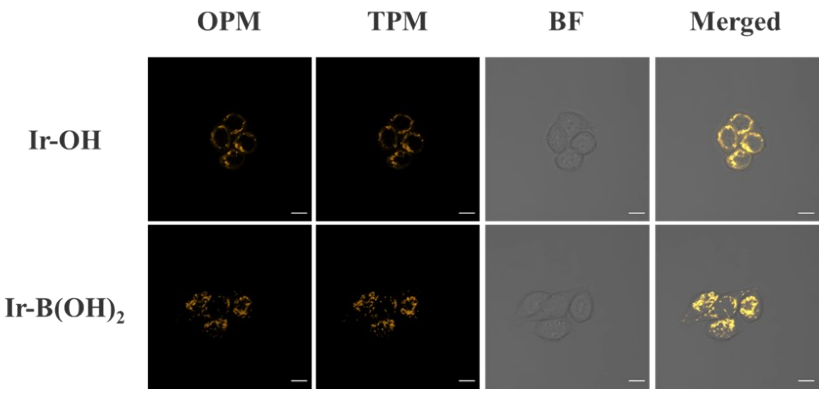

Figure S19. One and two-photon excited confocal laser scanning microscopy images of **Ir-OH** (0.5 μM) and **Ir-B(OH)$_2$** (0.5 μM) in AGS monolayer cells. Scale bar = 10 μm.

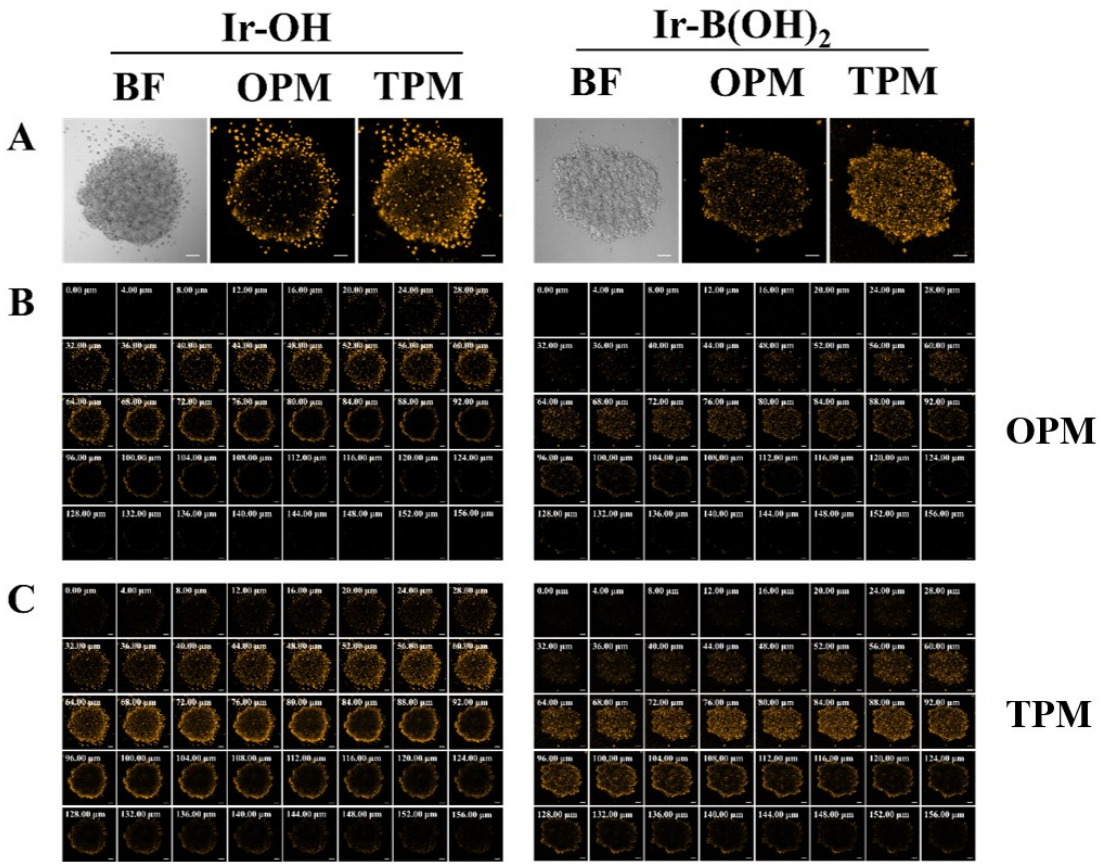

Figure S20. (A) One-photon (OPM) and two-photon (TPM) fluorescence microscopy images of **Ir-OH** (0.5 µM) and **Ir-B(OH)$_2$** (0.5 µM) in an intact 3D multi-cellular spheroid. Z-stack of (B) OPM and (C)TPM images of **Ir-OH** or **Ir-B(OH)$_2$** in AGS 3D multi-cellular spheroids. The images were taken every ~4.00 µm section along the Z axis of an intact spheroid. Scale bar = 100 µm.

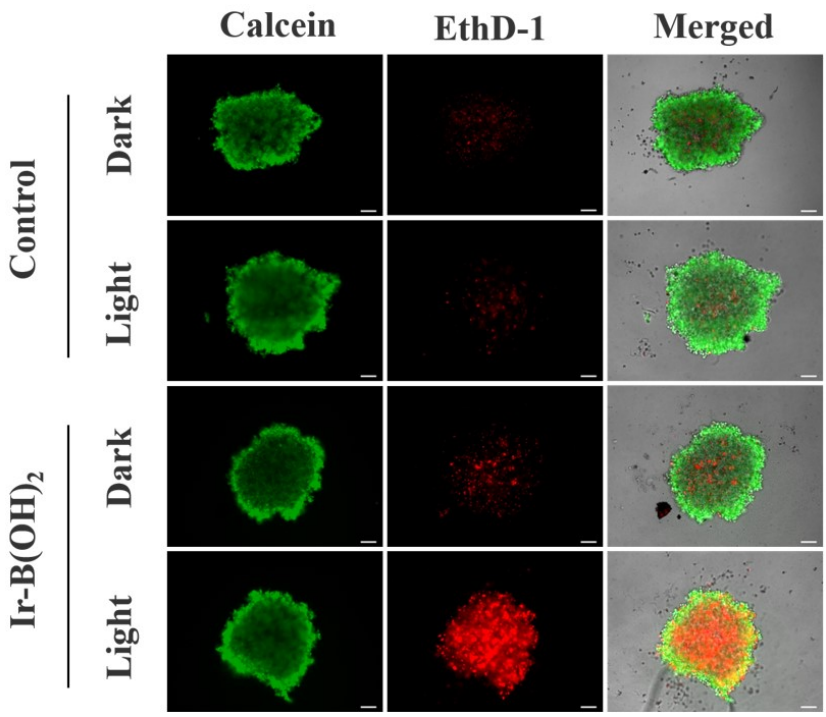

Figure S21. Fluorescence microscopy images of AGS MCTS incubated with **Ir-B(OH)$_2$** (0, 0.5 μM) upon treatment in the dark or exposure to a two-photon irradiation (730 nm, 20 mW cm^{-2}, 300 s). Afterwards the MCTS were stained with Calcein-AM/EthD-1 (Calcein-AM is a stain for living cells, 2μM, λ_{ex} = 488 nm, λ_{em} = 510 ± 10 nm; EthD-1 is a stain for dead cells, 4μM, λ_{ex} = 543 nm, λ_{em} = 610 ± 10 nm). Scale bar = 100 μm.

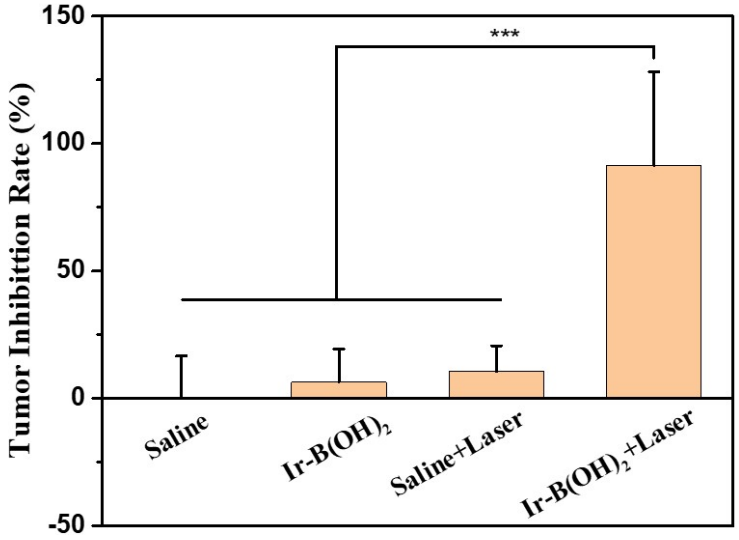

Figure S22. Change in tumor-inhibition rate after different treatments.

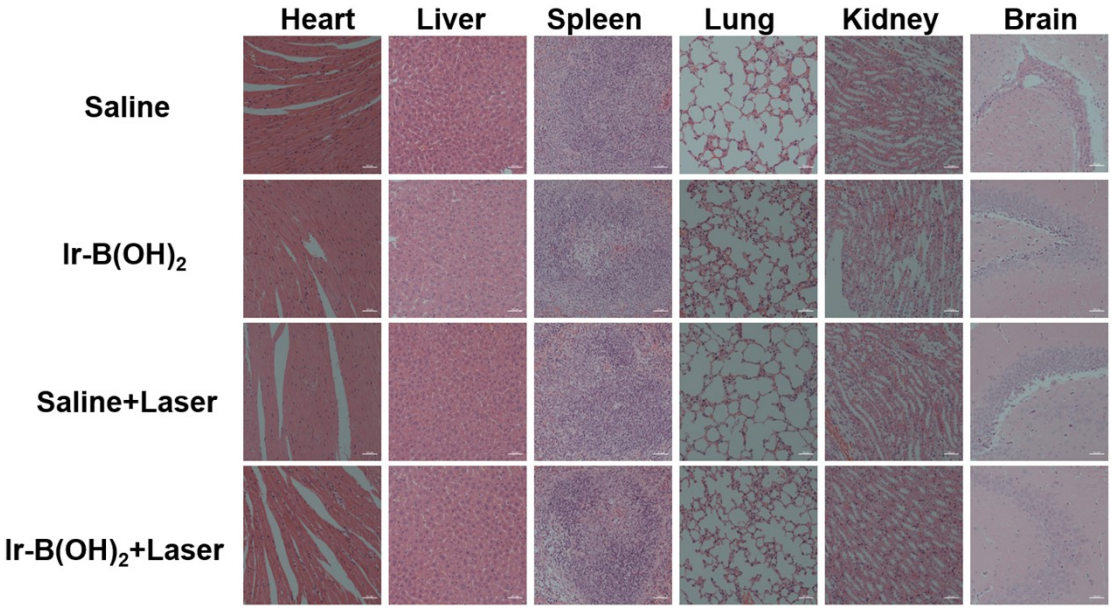

Figure S23. Histopathologic slices upon staining with hematoxylin and eosin (H&E) of the major organs (heart, liver, spleen, lung, kidney and brain) of AGS tumor-bearing mice after different treatments. Scale bar = 50 μm.

Table S1. (Photo)cytotoxicity towards different cell lines upon 405 nm laser irradiation.

Complexes		IC_{50} (μM)[a]			
		AGS	A549	Hela	L02
Ir-B(OH)$_2$	Dark	24±1.5	18 ±1.1	20±1.3	45±1.4
	Light	0.51±0.04	2.86±0.03	2.62±0.03	6.1±0.01
	PI	47	6.3	7.6	7.4
Cisplatin	Dark	24.6±1.1	21.2±1.1	15.4±0.7	15.9±0.8
	Light	23.4±1.3	22.1±0.9	14.8±1.3	16.1±0.7
	PI	1.1	0.95	1.0	0.99

[a] Data are presented as means ± s.d. (n=3).